

Manipulation of polyatomic molecules with the scanning tunnelling microscope at room temperature: chlorobenzene adsorption and desorption from Si(111)-(7 × 7)

This article has been downloaded from IOPscience. Please scroll down to see the full text article.

2006 J. Phys.: Condens. Matter 18 S1873

(<http://iopscience.iop.org/0953-8984/18/33/S07>)

View [the table of contents for this issue](#), or go to the [journal homepage](#) for more

Download details:

IP Address: 129.252.86.83

The article was downloaded on 28/05/2010 at 12:59

Please note that [terms and conditions apply](#).

# Manipulation of polyatomic molecules with the scanning tunnelling microscope at room temperature: chlorobenzene adsorption and desorption from Si(111)-(7 × 7)

P A Sloan<sup>1</sup> and R E Palmer

Nanoscale Physics Research Laboratory, School of Physics and Astronomy, University of Birmingham, Birmingham B15 2TT, UK

Received 4 November 2005, in final form 12 January 2006

Published 4 August 2006

Online at [stacks.iop.org/JPhysCM/18/S1873](http://stacks.iop.org/JPhysCM/18/S1873)

## Abstract

We report the imaging of chlorobenzene molecules chemisorbed on the Si(111)-(7 × 7) surface at room temperature with the scanning tunnelling microscope, and the desorption of the molecules by the tunnelling current. Detailed voltage-dependent imaging (at positive bias) allows the elucidation of the number and orientation of all the adsorbate configurations in the 7 × 7 unit cell. At negative bias the adsorbate was observed to affect the imaging properties of neighbouring half unit cells. The threshold voltage required for desorption of the chlorobenzene molecules was invariant to small changes in the tip-state, the adsorption site (corner adatom, middle adatom, faulted or unfaulted half of the unit cell) and the kind of doping of the substrate (n or p type).

## 1. Introduction

One of the ultimate aims of the growing field of nanoscience is the ‘complete’ control of matter on the atomic scale. The surface is the playground of atomic manipulation because it traps individual atoms or molecules for long enough to be probed, manipulated and probed again. The invention of the scanning tunnelling microscope (STM) [1] and subsequent work of Eigler and co-workers (see, e.g., [2–4]) proved that control of atoms and molecules on a metal surface was achievable. At low temperatures, the STM can be used to manipulate atoms in a controlled fashion through, for example, atomic scale displacement [5], dissociation of an individual chemical bond [6] or the creation of a chemical bond [7]. Recently, selective excitation of a particular vibrational mode has been used to regulate the ensuing molecular dynamics [8]. At room temperature, a more reactive surface has to be employed, often a semiconductor, to prevent atoms and small molecules from diffusing rapidly on the surface. This scenario poses

<sup>1</sup> Present address: Department of Chemistry, University of Toronto, 80 St George Street, Toronto, ON, M5S 3H6, Canada.

fresh challenges for atomic manipulation because the adsorbate/substrate bonding energies are much larger, typically a few electronvolts.

The manipulation of adsorbates on a semiconductor surface has seen a subtle development from atomic adsorbates and simple molecules [9, 10] to more complex molecules [11]. Even the relatively simple polyatomic molecule that we focus on here, chlorobenzene, exhibits a range of manipulation properties. Chlorobenzene can be desorbed from the Si(111)-(7 × 7) surface [12] but it can also undergo bond dissociation, e.g., by rupture of the C–Cl bond and ejection of a chlorine atom [13]. We have previously demonstrated a degree of control of the ejected chlorine atom in the dissociation reaction [14, 15], and tip-state control of the branching ratio between the two main competing manipulation channels, desorption and dissociation [16]. But in order to move towards full atomic scale control of matter, all the manipulation channels and possible environmental influences have to be mapped out.

In this paper we give a more detailed account of the adsorption of chlorobenzene on the Si(111)-(7 × 7) surface, as probed by STM, and the controlled desorption of the molecules initiated by the STM tunnelling current, as well as extending our work into new areas. We examine more closely the adsorption properties of chlorobenzene on Si(111)-(7 × 7). We show that a single adsorbate influences the imaging properties outside its own unit cell and that a single STM image can determine the number and orientation (within fourfold symmetry) of all chlorobenzene configurations believed to occur on Si(111)-(7 × 7). The desorption process is then examined with a set of STM tips that had similar imaging characteristics and investigated as a function of adsorption site and silicon doping. We found no major dependence of the desorption behaviour on these parameters, demonstrating the robust nature of the process.

## 2. Experimental details

In this section we describe some of the technical details underpinning the room temperature atomic manipulation experiments. The experiments were carried out in a UHV chamber with a base pressure of  $2 \times 10^{-10}$  Torr. The chamber was equipped with a room temperature STM with sample and tip transfer capabilities. The chamber also included a quadrupolar mass spectrometer, low energy electron diffraction apparatus and high resolution electron energy loss spectrometer. To minimize vibrations in the tunnel junction, the STM head was suspended in the chamber from low resonance frequency springs with eddy current damping. The chamber itself sat on a 10 tonne concrete block mounted on air legs and located inside an acoustically sealed booth.

Silicon(111) samples were cut from n-type (phosphorus doped) and p-type (boron doped) single-crystal wafers 0.38 mm thick with resistivities between 1 and 30  $\Omega$  cm. The cut samples were cleaned using ultrasonic agitation for five minutes in a bath of isopropanol and then a further five minutes in acetone. The samples were carefully dried to prevent ‘coffee-ring’ residue marks. Before entering vacuum, the samples were vigorously dusted with a flowing nitrogen gas jet.

Using resistive heating, the samples were degassed overnight at 700 °C before being flashed for 30 s at temperatures increasing up to 1300 °C, removing residual contamination and the native oxide layer. The final sample preparation step involved a flash to 1300 °C for 30 s, rapid cooling to 960 °C and then slower cooling at a rate of 1 °C s<sup>-1</sup> down to room temperature. This created extremely large (10 000 Å × 10 000 Å) and almost defect free Si(111)-(7 × 7) terraces.

High purity (99.9%) chlorobenzene liquid was subject to repeated freeze/pump/thaw cycles until all signs of contamination, as observed using mass spectrometry, were eliminated. To create a Si(111)-(7 × 7) surface partially covered with chlorobenzene molecules for desorption

experiments, a freshly cleaned surface was exposed to a small amount of chlorobenzene gas by back-filling the chamber with chlorobenzene vapour to a pressure of  $2 \times 10^{-8}$  Torr for 50 s. This dosage was designed to generate a surface coverage of  $\sim 1$  molecule per Si(111)-(7 × 7) unit cell.

The STM tips used for this work were made from 0.5 mm diameter polycrystalline tungsten wire. The tips were mounted in a tip-holder and ultrasonic agitation was used to clean the tip-wire/tip-holder assembly in a bath of isopropanol. To create the atomically sharp tip apex, a three-step electrochemical etch in 2 M NaOH with a 9 V potential was used incorporating the drop-off technique. First, to clean the tip-wire, a short etch, typically only 30 s long, was performed on the whole tip-wire. Second, a full etch to remove any cracked portion of the wire was conducted. Finally, another full etch was performed to create the STM tip apex. The tip was then transferred into the UHV chamber via a load-lock.

In the UHV system, electron bombardment was used to remove the residual tungsten oxide layer from the tip [17]. The tip was placed adjacent to a tungsten filament and a +100 V bias applied to the tip while a DC current passed through the filament. Hot electrons accelerated from the filament to the tip-apex locally heat the tip-apex. The degree of heating was increased stepwise by increasing the filament current. To prevent excessive melting of the tip-apex, the Fowler–Nordheim field emission characteristics were measured after each heating step [18]. The work-function of the tip-apex falls as the oxide layer is removed, resulting in an increase in the field-emission current at a particular voltage. Conversely, melting of the tip-apex results in a decrease of the emission current. Heating was stopped once the field-emission characteristics stopped improving and started to get worse. The most stable tips were produced by stripping the oxide layer and slightly melting the tip apex. The slightly rounded tip-apex of a partially melted tip may be less prone than an ultra-sharp tip to fatal bending if crashed into the surface.

The final stage of tip preparation was the iterative process of attaining an STM image that was both stable and reproducible. To induce small changes in the tip-apex, a short voltage pulse (−4 V for 20 ms) was applied to the sample. It is thought that such pulses may induce a single silicon atom to jump from the surface onto the tip-apex [19]. This pulsing procedure was repeated until the tip imaged in the desired fashion. In [16] we reported for chlorobenzene chemisorbed on Si(111)-(7 × 7) two distinct, stable and reproducible states of the tip: one that imaged chlorobenzene as a bright feature (termed a bright tip), and the other that imaged chlorobenzene as a dark feature (termed a dark tip). Switching between states was either initiated using the above pulsing method, or occurred spontaneously while scanning the surface. Once produced, either spontaneously or by pulsing, both tip-states were stable for  $\sim 30$  min, enough time to perform several manipulation experiments. Both tip-states induced desorption and dissociation, but with differing yields and differing branching ratios. We suggested that these differences were due to the coupling efficiencies of the tip to the  $\pi$  (and  $\pi^*$ ) states of the molecule. In this paper, to study adsorption we examine STM images taken with the dark-tip state. However, because of the greater probability of inducing desorption with a bright tip, the desorption results reported here were from experiments using the bright-tip state.

### 3. Adsorption

When chlorobenzene chemisorbs on the Si(111)-(7 × 7) surface, the aromatic nature of the ring is lost and a cyclohexadiene-like, 2,5 di- $\sigma$  bonded butterfly structure is formed [12, 20]. Two  $sp^3$  carbon atoms on opposite sides of the ring bond to an adatom/rest-atom pair of silicon atoms, leaving two pairs of  $sp^2$  carbon atoms on each wing of the adsorbed molecule. At +1 V sample bias, the signature of these chemisorbed chlorobenzene molecules on Si(111)-(7 × 7) is

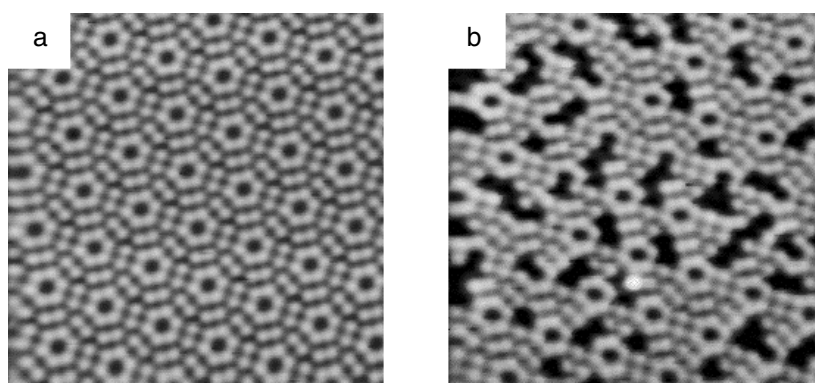


**Figure 1.** STM images (in both cases the same sample bias +1 V, tunnelling current 50 pA and image size  $150 \text{ \AA} \times 150 \text{ \AA}$ ). Taken (a) before chlorobenzene gas has been dosed onto a Si(111)-(7  $\times$  7) surface and (b) after chlorobenzene dosing ( $150 \times 10^{-8}$  Torr s).

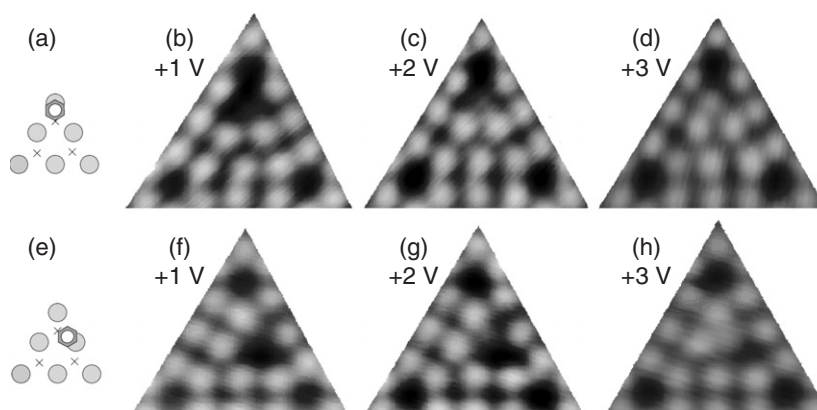


**Figure 2.** STM images, and schematic diagram, of half the  $7 \times 7$  unit cell for chlorobenzene/Si(111)-(7  $\times$  7) as a function of sample bias voltage. (a)–(d) Chlorobenzene bonded to a corner-adatom and rest-atom pair, bias voltages as marked. (e)–(h) Chlorobenzene bonded to a middle-adatom and rest-atom pair, bias voltages as marked. All images taken with 100 pA tunnelling current.

a missing-adatom-like feature. Figure 1 shows two STM images, both obtained at +1 V, before (a) and after (b) exposure to chlorobenzene molecules. The darkening of particular adatoms is due to the saturation of the dangling bond upon chemisorption to the adsorbate. Indeed, missing-adatom features are the STM imaging signatures of many species that chemisorb on the Si(111)-(7  $\times$  7) surface, from small adsorbates such as NO [21], HBO<sub>2</sub> [22] and ethylene [23], to larger adsorbates such as the dienes [24] and other more complex molecules (see, e.g., [25]). At +1 V bias voltage no intra-molecular features are imaged by the STM (figures 2(b) and (f)).

Above a sample bias voltage of +1 V, a bright feature grows above the location of the silicon rest-atom to which the chlorobenzene is bonded, irrespective of whether the molecule is bonded to a corner-adatom (figures 2(c) and (d)) or to a middle-adatom (figures 2(g) and (h)). This bright feature, observed at +2 V in figures 2(c) and (g) brightens further at +3 V, figures 2(d) and (h). We have previously speculated that the bright feature is due to resonant tunnelling through the  $\pi^*$  state of the molecule [16]. At +3 V, the neighbouring adatoms are also slightly brightened, possibly due to charge transfer away from these adatom sites induced

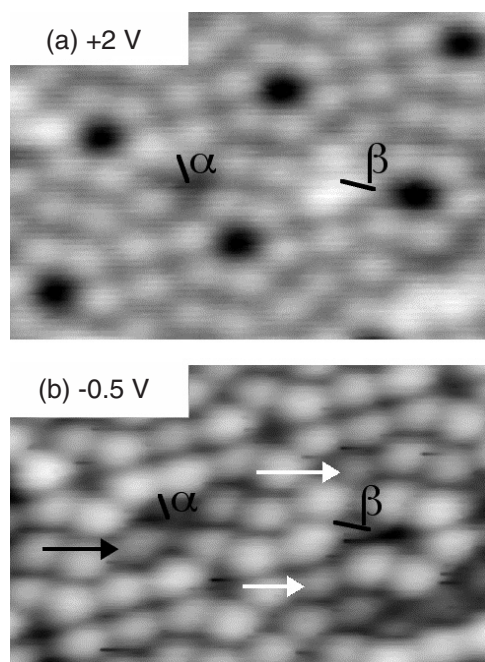


**Figure 3.** (a) STM image ( $60 \text{ \AA} \times 40 \text{ \AA}$ , 50 pA) taken at +2 V of a Si(111)-(7 × 7) surface with the adatom–rest-atom axis of two chlorobenzene adsorbates indicated by black lines:  $\alpha$ , a chlorobenzene bonded to a middle-adatom and rest-atom pair;  $\beta$ , a chlorobenzene bonded to a corner-adatom and rest-atom pair. (b) STM image ( $60 \text{ \AA} \times 40 \text{ \AA}$ , 50 pA) of the same area as (a) but with  $-0.5 \text{ V}$  bias. Chlorobenzene molecules marked as before. The black arrow points to a neighbouring adatom of the middle-adatom bonded molecule that is darkened. The two white arrows point to a pair of neighbouring adatoms to the corner-bonded molecule that are both darkened.

by the chemisorbed molecule [26]. A molecule bonded to a middle adatom has a choice of two neighbouring rest-atoms. The brightening of the relevant bonding rest-atom allows us to determine the orientation of the ring. However, we do not know the precise location of the chlorine atom, just that it is attached to one of the four carbon atoms not bonded to the surface [20].

Figure 3 shows a pair of STM images, (a) taken with +2 V and (b) with  $-0.5 \text{ V}$ , of the same area of surface with two chlorobenzene adsorbates. The orientation of an adatom–rest-atom pair, determined from the +2 V image, is indicated for both molecules:  $\alpha$  labels the chlorobenzene molecule bonded to a middle-adatom and rest-atom pair;  $\beta$  labels a chlorobenzene molecule bonded to a corner-adatom and rest-atom pair. In a similar fashion to the positive-bias imaging, at negative bias the adatom that bonds to the molecule images as a dark missing-adatom-like feature. The covalent bond between surface and adsorbate lowers the bonding electrons' binding-energy, therefore these electrons are not imaged by the STM at small negative bias [26].

Figure 3(b) also reveals that chlorobenzene adsorbates modify not only the half unit cell that the adsorbate is attached to, but also the neighbouring half unit cells. As far as we are aware, this is the first report of an adsorbate affecting the STM imaging properties of the Si(111)-(7 × 7) surface outside the bonding half unit cell. As indicated by the black arrow in figure 3(b), the middle-adatom bonded molecule ( $\alpha$ ) depresses the middle adatom of the

adjacent half unit cell ( $-1.5 \text{ \AA}$  relative to a normal adatom). As indicated by the white arrows in figure 3(b), the corner-adatom bonded molecule ( $\beta$ ) depresses two middle adatoms, one in each of the two adjacent half unit cells ( $-1 \text{ \AA}$  relative to a normal adatom). We now discuss possible causes for this darkening.

The contrast of an STM image is primarily controlled by two properties of the surface, electronic and physical (height). A change in either one of these properties will lead to a change in the imaged STM contrast (the measured height). The clean Si(111)-( $7 \times 7$ ) unit cell itself exhibits complex electronic structure. For example, there is charge redistribution between the adatoms and rest-atoms of a half unit cell; the adatoms donate most of their unpaired electron to their neighbouring rest-atoms [27, 28]. This charge redistribution can be perturbed by the presence of a chemisorbed adsorbate, and hence the appearance of the relevant adatoms in an STM image [26]. Between half unit cells there are no linking rest-atoms and so a different route for charge redistribution would be needed to account for the observed darkening of the adatoms in this work.

Another possible cause for the observed darkening is charge redistribution induced by the dipole moment of the C–Cl bond. As the chlorine atom is bonded to one of the non-surface-bonded carbon atoms [20] there should be an asymmetry, relative to the adatom–rest-atom axis of the adsorbate, in any dipole field generated by the C–Cl bond. However, figure 3(b) clearly demonstrates that the corner-adatom-bonded molecule generates a symmetric pattern on either side of the adatom–rest-atom axis, and so it seems unlikely that long-range effects of the C–Cl dipole are the cause of the depressions.

Instead, the darkening of the neighbouring adatom could be a physical property, i.e., the darkened adatom may simply be lower than a clean adatom. As evident by its small desorption energy of  $\sim 1 \text{ eV}$ , chlorobenzene chemisorbs to the Si(111)-( $7 \times 7$ ) surface in a highly strained di- $\sigma$  bonded configuration [20]. The strained molecular configuration may be mirrored by a local surface reconstruction.

We note finally in this discussion that the darkening is visible at negative polarity but not at positive polarity, the same asymmetry as found for the STM imaging properties associated with the stacking fault of the Si(111)-( $7 \times 7$ ) surface: at negative bias the faulted half of the unit cell images brighter than the unfaulted half; at positive bias this difference is not observed [27]. This similarity may tend to suggest that electronic effects do play at least some role in the adjacent adatom darkening effect.

Chlorobenzene adsorption is of course not restricted to a single molecule per half unit cell; there can be two (figures 4(a)–(e)) or three (figures 4(f)–(j)) molecules in a half unit cell. Assuming a di- $\sigma$  bonding configuration, figure 4 presents all the possible adsorption combinations for more than one chlorobenzene molecule per half unit cell of the Si(111)-( $7 \times 7$ ) surface. In principle, the location and orientation (within fourfold symmetry) of every chlorobenzene configuration believed to occur on the Si(111)-( $7 \times 7$ ) surface can therefore be determined. This capability proves crucial when examining the STM induced C–Cl bond dissociation mechanism [15].

#### 4. Desorption

Figures 5(a) and (b) are a pair of STM images ( $100 \text{ \AA} \times 100 \text{ \AA}$ ) which were obtained with tunnelling parameters chosen not to disturb the system (sample bias +1 V, tunnelling current 50 pA). These images show the same area and were taken before (a) and after (b) scanning the area under tunnelling conditions that lead to some desorption of the chlorobenzene molecules (in this case, the manipulation parameters were a sample bias voltage of +2.2 V and a tunnelling current of 50 pA). As illustrated by the sites circled in the two figures, it is evident

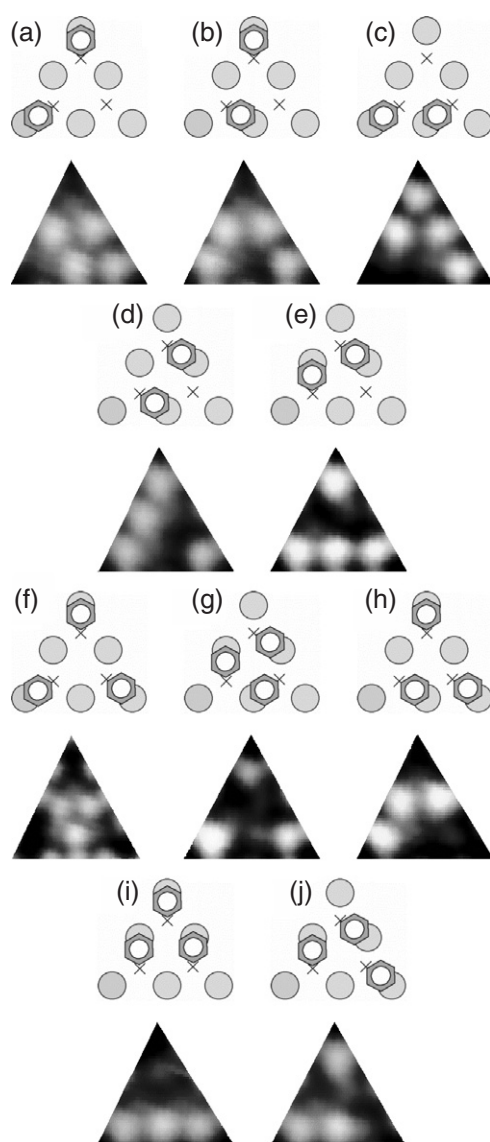


**Figure 4.** STM images (all +2 V and 100 pA) with corresponding schematics of all the possible chlorobenzene bonding configuration in a half Si(111)-(7 × 7) unit cell; (a)–(e) for two adsorbates, (f)–(j) for three adsorbates.

that the number of chemisorbed chlorobenzene molecules, that appear like missing adatoms, is reduced in figure 5(b) compared with figure 5(a).

Another way of illustrating desorption involves imaging a larger area of the surface after a smaller area is scanned with tunnelling parameters which induce desorption. Figure 5(c) shows a 500 Å × 500 Å scan after the central square (outlined) of size 150 Å × 150 Å has been scanned (+3 V and 50 pA). Clearly evident in figure 5(c) is the cleaned area of the surface from which chlorobenzene molecules have been desorbed.

In figure 5(c) there is no evidence that the chlorobenzene molecules are swept along by the tip (which sweeps from right to left over the surface). Had such a mechanism occurred,



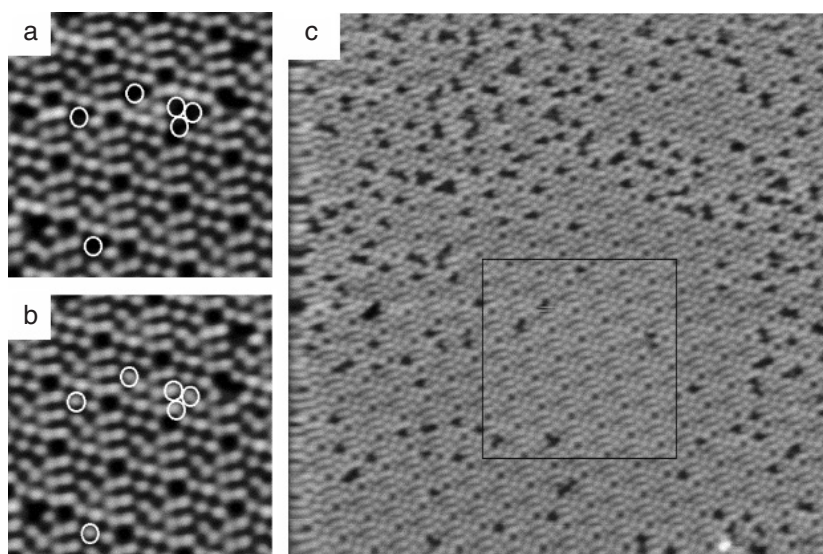


**Figure 5.** STM images ( $100 \text{ \AA} \times 100 \text{ \AA}$ ) of chlorobenzene molecules on Si(111)-(7  $\times$  7) before (a) and after (b) a desorption scan. Image parameters: sample bias +1 V and tunnelling current 50 pA. The white circles mark the locations of chlorobenzene molecules which desorb in this case. (c) STM image ( $500 \text{ \AA} \times 500 \text{ \AA}$ , +1 V, 50 pA) of chlorobenzene on Si(111)-(7  $\times$  7) after previous scanning of a  $150 \text{ \AA} \times 150 \text{ \AA}$  area (marked square) to induce chlorobenzene desorption (+3 V and 50 pA).

one would expect chlorobenzene molecules to be piled up at the right and left hand edges of the marked square. Sweeping effects such as pulling, pushing and sliding have been reported in numerous other manipulation experiments [5], typically for adsorbates (large and small) physisorbed at cryogenic temperatures on metallic surfaces [29]. Small molecule manipulation generally uses the attractive force which exists between the tip and adsorbate to overcome the small surface corrugation of a metallic surface, whereas larger molecules usually exploit the larger repulsive forces in action when a tip pushes molecules across a surface. However, due to the chemisorbed nature of chlorobenzene on the Si(111)-(7  $\times$  7) surface, there will be a large energy barrier to lateral movement similar to the desorption energy of  $\sim 1.0 \text{ eV}$  [20]. This is because the adsorbate/surface covalent bonds would need to be broken and remade at every step, thereby precluding sweeping of the molecule by the STM tip. Adsorbate chemisorption on the Si(111)-(7  $\times$  7) surface does not necessarily prevent sweeping effects. For example, if the molecule is large enough to allow the tip to push it and large enough to remain chemisorbed throughout the sweeping process, as is the case for  $\text{C}_{60}$  on Si(111)-(7  $\times$  7) [30], then the STM tip can sweep the adsorbate.

The acquisition of numerous image pairs similar to those in figures 5(a) and (b) (typically over an area of  $500 \text{ \AA} \times 500 \text{ \AA}$ ) obtained with a wide range of manipulation parameters allows the simple counting of the number of desorbed molecules. Such data can be used to plot the desorption probability [31] as a function of both current and voltage, and also to derive the desorption rate as a function of current or tip-to-surface height.

To calculate the desorption rate, three parameters are required from each image pair; the initial number of chlorobenzene molecules in the scan before manipulation; the final number of chlorobenzene molecules in the scan after manipulation; and the time the tip spends over each chlorobenzene molecule during the manipulation scan. Assuming a first order rate process,

the desorption rate (desorption events per unit time) and the desorption yield (desorption events per tunnelling electron) can be calculated.

To count the number of chlorobenzene molecules on the surface before a manipulation scan, the target area was initially scanned at +1 V, 50 pA and then immediately after this at +2 V, 50 pA. Similar scans were taken after the manipulation scan. These imaging parameters were chosen specifically so that there was a minimal probability of any desorption occurring during these scans. Any change in the number of adsorbed chlorobenzene molecules could therefore be attributed to the manipulation scan itself. It was necessary to scan at both +1 and +2 V before and after the manipulation scan as this enabled the identification, through their imaging properties, of adsorbed chlorobenzene, missing adatoms and contamination features. Silicon adatoms image bright at both voltages, missing adatoms image dark at both voltages and chlorobenzene images dark at +1 V and brighter at +2 V. Knowing the total scan time and assuming an area for an adsorbed chlorobenzene molecule of  $25 \text{ \AA}^2$  [31], the time the tip spent over an individual chlorobenzene could be calculated and hence the desorption rate and yield derived.

Before describing the new results presented in this paper, we briefly review our previously published work on the STM-induced desorption of chlorobenzene from Si(111)-(7 × 7) [12]. We carried out a systematic experimental investigation of the mechanism of this process. Measurements of the desorption yield over a wide range of both positive and negative sample bias voltages (from -3 to +4 V) established asymmetric threshold voltages for desorption (figure 6(a)). Measurements as a function of tunnelling current (figures 6(b) and (c)) ruled out vibrational heating, electric field and mechanical (i.e., tip-surface force) mechanisms. We deduced that the desorption was driven by the population of negative (or positive) ion resonance states of the chemisorbed chlorobenzene molecule [32]. Comparison with the density of states calculated using density functional theory led to the further proposal that these resonance states are the  $\pi^*$  (or  $\pi$ ) orbitals of the chlorobenzene adsorbate. In this paper we discuss in detail the effect on desorption of (i) small changes in the tip-state, (ii) the adsorption site and (iii) the doping of the silicon substrate.

One of the most crucial, yet relatively uncontrolled and unknown, aspects of any STM experiment is the state of the tip. At low temperatures a few groups have managed to pick up an individual atom or molecule and so perform experiments with (comparatively) well defined tip apexes [6, 7]. At room temperature, however, this level of control has not been achieved. Instead, the main aim has been to prevent the nature of the tip from playing too active a role in the manipulation process (e.g., by changing its configuration). This is approached in two ways: (i) by seeking to ensure that each tip used images the surface/adsorbate in approximately the same manner and (ii) by repeating the same experiment with many such tips [33].

Although in our experiments with chlorobenzene/Si(111)-(7 × 7) care was taken to ensure that the tip states are similar, e.g., by making sure that the surface imaged in a reproducible and standard fashion; there will always be small disparities in the STM images obtained with different tips. A new (different) tip state can arise for a number of reasons: a physically new tip is used; the same tip is used, but on a different day; or simply that while scanning the tip undergoes a change (e.g., because of a tip crash) which alters the atomic arrangement and/or composition at the tip apex.

The two STM images in figures 5(a) and (b) were taken before and after a manipulation scan and the imaging properties of the tip can be seen to be identical in both images. The same atomic tip apex produced these images. By contrast, in figures 1(a) and (b), where at first glance the Si(111)-(7 × 7) surfaces look identical (ignoring the chlorobenzene adsorbates) the adatoms in figure 1(a) are actually slightly smaller than in figure 1(b). The tip configuration that imaged figure 1(a) exhibited a better spatial resolution than the one that

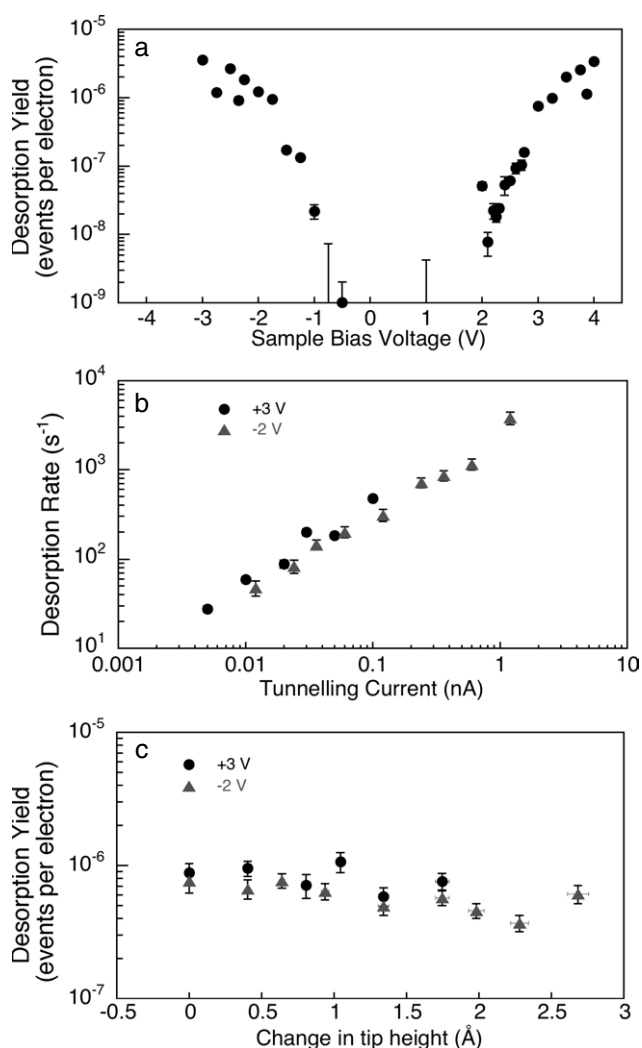


**Figure 6.** (a) Desorption yield (events per electron) of chlorobenzene molecules from the Si(111)-(7 × 7) surface as a function of the sample bias voltage in the STM. (b) Rate of desorption of chlorobenzene from the Si(111)-(7 × 7) surface as a function of the tunnelling current (log–log plot); sample bias +3 V (●) and –2 V (▲). (c) The same basic data as (b), plotted as desorption yield versus the change in tip–surface distance which occurs when the current is altered (positive value, tip moves towards the surface). The reference set points are +3 V, 5 pA (●) and –2 V, 10 pA (▲).

produced figure 1(b). This is not too surprising when it is revealed that these two images were taken months apart. Although the two different tips were cajoled to image the Si(111)-(7 × 7) in the same manner, there are always slight discrepancies when comparing different tips. We have recently shown that large differences in the imaging properties of different STM tips lead to large changes in the corresponding chlorobenzene behaviour [16], but what of the subtle differences in the imaging properties of the tips? Do they manifest themselves in the STM desorption process?

The obvious way to address this question is to carry out the same experiment many times with tips that image chlorobenzene/Si(111)-(7 × 7) in approximately the same fashion.

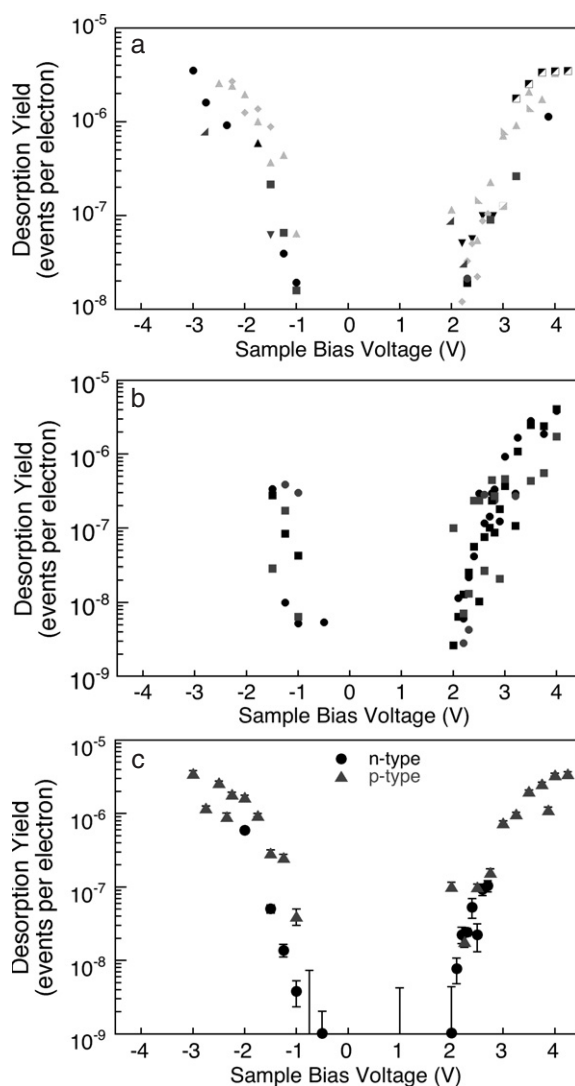


**Figure 7.** (a) Desorption yield of chlorobenzene from the Si(111)-(7 × 7) surface as a function of the voltage for 16 different STM tips. Each type of marker represents the data taken with one particular tip (see main text). (b) Desorption yield versus sample bias for four different adsorption sites: faulted corner (black ●) and unfaulted corner (grey ●); faulted middle (black ■), unfaulted middle (grey ■). (c) Desorption yield versus the sample bias for two different kinds of doping of the Si(111)-(7 × 7) substrate: n-type  $2 \times 10^{14}$ – $7 \times 10^{15}$  cm $^{-3}$  (●); p-type  $8 \times 10^{14}$ – $2 \times 10^{16}$  cm $^{-3}$  (▲).

Figure 7(a) shows the same data from figure 6(a) but broken down into sets corresponding to the 16 individual tips used in these experiments. Apparent are the modest differences in the desorption yields from tip to tip at the same desorption voltage ( $\pm 40\%$ ). These differences are small when compared with the three orders of magnitude change in the yield that take place over the bias range probed. Consequently, although the exact nature of the tip may to some extent influence the desorption yield, the process of desorption remains largely unaffected by the slight differences between different tips prepared according to the same recipe. The absolute value

of the desorption probability fluctuates due to subtle differences between the STM tips, but the overall trend in the yield over the wide bias range explored is unaffected by such fluctuations. Similar observations have been reported in other manipulation experiments [2, 19].

The desorption yield is affected through a major change in the tip e.g., from a bright tip to a dark tip [16]. Both tip-states exhibited a +3 V onset for desorption, indicating that the  $\pi$  states of the molecule mediate desorption in each case. A change in the tip-state did, however, change the absolute rate of desorption. There was a factor  $50 \pm 10$  difference between bright-tip and dark-tip induced desorption. The higher rate of desorption was produced by the bright tip, and as desorption is mediated by the  $\pi$  states we associated the bright tip with a higher probability of tunnelling electrons into (and out of) the  $\pi$  states of the molecule. This leads to the increase in the imaged height and the increase in desorption yield relative to the dark tip. The STM tip influences the cross-section for a tunnelling electron to induce desorption, but not the desorption process itself.

The (bias-dependent) desorption yield of chlorobenzene from Si(111)-(7 × 7) was also explored as a function of the molecular adsorption site. Within the statistical noise level shown in figure 7(b), no differences were observed between corner or middle adatom sites, or between the faulted and unfaulted halves of the unit cell. Similar behaviour was found for the dissociation of HS and DS on the Si(111)-(7 × 7) surface [34]. In our experiments, we have a threshold behaviour of our STM induced desorption due to the onset of resonant tunnelling into (or out of) the  $\pi^*$  ( $\pi$ ) states of the molecule [12]. At both polarities the energy of the  $\pi$  states ( $>1.5$  eV) is higher than the desorption energy of chlorobenzene ( $\sim 1.0$  eV [20]). Our findings are therefore evidence that at each adsorption site (corner or middle adatom) and each half of the unit cell (faulted or unfaulted) the electronic structures of the  $\pi$  and  $\pi^*$  states of the chemisorbed chlorobenzene molecule are the same. This is consistent with the idea that all adsorption sites involve the same geometry of adatom/rest-atom pair and (within experimental error [20]) have the same adsorption energy.

An interesting approach that has been mooted [35] to facilitate resonant manipulation experiments is to change the dopant (n to p, or vice versa) of a semiconductor substrate and examine the bias dependence of the manipulation process. Figure 7(c) shows the bias dependence of the desorption yield of chlorobenzene from Si(111)-(7 × 7) on lightly doped boron p-type ( $8 \times 10^{14}$ – $2 \times 10^{16}$  cm<sup>-3</sup>) and phosphorus n-type ( $2 \times 10^{14}$ – $7 \times 10^{15}$  cm<sup>-3</sup>) silicon. Immediately apparent is that the onset of desorption is the same in both cases. This means that the energy offsets between the  $\pi$  and  $\pi^*$  states and to the Fermi level are unchanged by the change in doping. As the surface is only partially covered by chlorobenzene molecules and the doping is relatively light, the Fermi level would be pinned mid-gap in both cases, leading to the same energy differences between the Fermi level and the  $\pi/\pi^*$  states. If, on the other hand, a fully saturated surface [33] or a heavily doped crystal [36] were used, then we might expect to observe some shift in the bias voltage thresholds.

## Acknowledgments

We thank the EPSRC and the European Research Training Networks ‘Manipulation of individual atoms and molecules’ and ‘AMMIST’ for financial support of this work. PAS acknowledges studentship support from the School of Physics and Astronomy and the EPSRC. PAS also thanks Dr S E A Birse for critical reading of this manuscript.

## References

- [1] Binnig G, Rohrer H, Gerber C and Weibel E 1982 *Appl. Phys. Lett.* **40** 178
- [2] Eigler D M and Schweizer E K 1990 *Nature* **344** 524

- [3] Eigler D M, Lutz C P and Rudge W E 1991 *Nature* **352** 600
- [4] Heinrich J A, Lutz C P, Gupta J A and Eigler D M 2002 *Science* **298** 1381
- [5] Bartels L, Meyer G and Rieder K H 1997 *Phys. Rev. Lett.* **79** 697
- [6] Hla S W, Bartels L, Meyer G and Rieder K H 2000 *Phys. Rev. Lett.* **85** 2777
- [7] Hahn J R and Ho W 2001 *Phys. Rev. Lett.* **87** 166102
- [8] Pascual J I, Lorente N, Song Z, Conrad H and Rust H P 2003 *Nature* **423** 525
- [9] Shen T C *et al* 1995 *Science* **268** 1590
- [10] Quaade U, Stokbro K, Thirstrup C and Grey F 1998 *Surf. Sci.* **415** L1037
- [11] Lastapis M, Martin M, Riedel D, Hellner L, Comtet G and Dujardin G 2005 *Science* **308** 1000
- [12] Sloan P A, Hedouin M F G, Palmer R E and Persson M 2003 *Phys. Rev. Lett.* **91** 118301
- [13] Lu P H, Polanyi J C and Rogers D 1999 *J. Chem. Phys.* **111** 9905
- [14] Palmer R E, Sloan P A and Xirouchaki C 2004 *Phil. Trans. R. Soc. A* **362** 1195
- [15] Sloan P A and Palmer R E 2005 *Nature* **434** 367
- [16] Sloan P A and Palmer R E 2005 *Nano Lett.* **5** 835
- [17] Chen C J 1993 *Introduction to Scanning Tunneling Microscopy* (Oxford: Oxford University press)
- [18] Fowler R H and Nordheim W L 1928 *Proc. R. Soc. A* **119** 173
- [19] Kobayashi A, Grey F, Williams R S and Aono M 1993 *Science* **259** 1724
- [20] Cao Y, Deng J F and Xu G Q 2000 *J. Chem. Phys.* **112** 4759
- [21] Rezaei M A, Stipe B C and Ho W 1999 *J. Chem. Phys.* **110** 4891
- [22] Miyake K, Ishida M and Shigekawa H 1998 *Appl. Surf. Sci.* **130–132** 78
- [23] Piancastelli M N, Motta N, Sgarlata A, Balzarotti A and Decrescenzi M 1993 *Phys. Rev. B* **48** 17892
- [24] Shachal D, Manassen Y and TerOvanesyan E 1997 *Phys. Rev. B* **55** 9367
- [25] Fukuda Y, Shimomura M, Kaneda G, Sanada N, Zavodinsky V G, Kuyanov I A and Chukurov E N 1999 *Surf. Sci.* **442** 507
- [26] Avouris P and Wolkow R 1989 *Phys. Rev. B* **39** 5091
- [27] Hamers R J, Tromp R M and Demuth J E 1986 *Phys. Rev. Lett.* **56** 1972
- [28] Northrup J E 1986 *Phys. Rev. Lett.* **57** 154
- [29] Gauthier S 2000 *Appl. Surf. Sci.* **164** 84
- [30] Beton P H, Dunn A W and Moriarty P 1995 *Appl. Phys. Lett.* **67** 1075
- [31] Alavi S, Rousseau R, Patitsas S N, Lopinski G P, Wolkow R A and Seideman T 2000 *Phys. Rev. Lett.* **85** 5372
- [32] Salam G P, Persson M and Palmer R E 1994 *Phys. Rev. B* **49** 10655
- [33] Soukiasian L, Mayne A J, Carbone M and Dujardin G 2003 *Phys. Rev. B* **68** 035303
- [34] Rezaei M A, Stipe B C and Ho W 1998 *J. Chem. Phys.* **109** 6075
- [35] Patitsas S N, Lopinski G P, Hul'ko O, Moffatt D J and Wolkow R A 2000 *Surf. Sci.* **457** L425
- [36] Piva P G *et al* 2005 *Nature* **435** 658